Biological Journal of the Linnean Society, 2017, **121**, 627–640. With 6 figures.

Genetic diversity and Quaternary range dynamics in Iranian and Transcaucasian tortoises

HOSSEIN JAVANBAKHT[1], FLORA IHLOW[2], DANIEL JABLONSKI[3], PAVEL ŠIROKÝ[4], UWE FRITZ[5], DENNIS RÖDDER[2], MOZAFAR SHARIFI[6] and PETER MIKULÍČEK[3*]

[1]*Department of Biology, Faculty of Sciences, University of Guilan, Rasht, Iran*
[2]*Herpetology Section, Zoologisches Forschungsmuseum Alexander Koenig (ZFMK), Adenauerallee 160, 53113, Bonn, Germany*
[3]*Department of Zoology, Faculty of Natural Sciences, Comenius University in Bratislava, Mlynská dolina, Ilkovičova 6, 842 15 Bratislava, Slovak Republic*
[4]*Department of Biology and Wildlife Diseases, Faculty of Veterinary Hygiene and Ecology, University of Veterinary and Pharmaceutical Sciences Brno, Palackého tř. 1/3, 61242 Brno, Czech Republic*
[5]*Museum of Zoology, Senckenberg Dresden, A. B. Meyer Building, 01109 Dresden, Germany*
[6]*Department of Biology, Faculty of Science, Bagabrisham 6714967346, Razi University, Kermanshah, Iran*

Received 11 November 2016; revised 24 December 2016; accepted for publication 5 January 2017

The range dynamics of species distributed in temperate zones was significantly influenced by climatic fluctuations during the Pleistocene. However, little is known on how glacial and interglacial cycles affected the distribution of species occupying lower latitudes. The aim of this study was to assess Quaternary range dynamics of the spur-thighed tortoise (*Testudo graeca*) in Iran and Transcaucasia and to infer how range fluctuations influenced the species' genetic diversity. We analysed mitochondrial DNA variation of samples from Iran and Transcaucasia and reconstructed the species' palaeogeography by projecting species distribution models (SDMs) onto palaeoclimatic conditions of the mid-Holocene (6000 BP) and the Last Glacial Maximum (LGM, 21 000 BP). We found three mitochondrial lineages in Iran, corresponding to the subspecies *T. g. armeniaca*, *T. g. buxtoni* and *T. g. zarudnyi*, whose current distribution is limited predominately by precipitation. A combination of SDMs and demographic analyses revealed that the ranges of these subspecies experienced only a slight shift during the Quaternary and did not expand significantly after the LGM. These results for *T. graeca* indicate that range dynamics of ectothermic taxa occupying lower latitudes in the western Palaearctic might be more complex and may not follow a simplistic scenario of glacial retraction and postglacial expansion.

ADDITIONAL KEYWORDS: historical biogeography – Middle East – mitochondrial DNA – phylogeography – Pleistocene climatic fluctuations – species distribution model (SDM) – Testudines – Testudinidae – *Testudo graeca*.

INTRODUCTION

Genetic diversity and distribution ranges of organisms living in the temperate zone were significantly affected by climatic oscillations during the Pleistocene. A cycle of repeating glacial and interglacial periods led to range contractions and expansions as climatic and environmental conditions were changing (Avise, 2000; Hewitt, 2000; Schmitt, 2007). During cold periods, the ranges of thermophilic plant and animal species contracted to climatically favourable areas (refugia) in the south, while these taxa were able to expand their ranges during warm periods considerably to the north. In Europe such areas were mainly located in the southern peninsulas (Taberlet *et al.*, 1998). Long-term persistence of populations in southern refugia induced genetic differentiation and eventually led to high genetic and taxonomic diversity. On the other hand,

*Corresponding author. E-mail: pmikulicek@fns.uniba.sk

postglacial expansion from refugia and rapid colonization of the north produced areas with reduced genetic diversity. Pleistocene range dynamics and their genetic consequences have been studied in many temperate species (Hewitt, 2011), while the influence of glaciations on range dynamics and genetic diversity in other parts of the world remains largely unknown. The classical scenario proposed for higher latitudes appears too simplistic for lower latitudes where more complex responses to climate changes and range dynamics are to be expected (Médail & Diadema, 2009). Apart from postglacial expansion, these include contraction, shift and stability of ranges (Anadón *et al.*, 2015). In this paper we focus on the biogeographical history of tortoises living in Iran and Transcaucasia to determine how their Middle Eastern ranges have been affected by Quaternary climatic fluctuations.

Tortoises are an ideally suited model for studying range dynamics of thermophilic species because they are slow dispersers, which is why their genetic structure is expected to be more influenced by range contractions than in rapidly dispersing taxa. In rapid dispersers, gene flow is expected at a higher rate during interglacial periods, sweeping out or mitigating signatures of former range interruptions. In the Western Palaearctic, the spur-thighed tortoise, *Testudo graeca* Linnaeus, 1758 (Testudinidae: Testudines), represents the most widely distributed species of tortoise, ranging from Morocco to eastern Iran (Fritz & Havaš, 2007; Fritz *et al.*, 2007, 2009). Within this wide range, the species exhibits substantial morphological and genetic diversity. Phenotypic plasticity and adaptation to local environments caused extensive variation in size, shape and colour of the shell, which conflicts with significantly less pronounced phylogeographical differentiation (Fritz *et al.*, 2007, 2009; Mikulíček *et al.*, 2013). With respect to mitochondrial DNA (mtDNA), Fritz *et al.* (2007, 2009) recognized six main lineages within *T. graeca*, which were suggested to have diverged 4.2–1.8 Mya (Fritz *et al.*, 2009). In the Caucasus region, extensive gene flow among the lineages with abutting distributions has been recorded, indicating the lack of effective reproductive isolation and, under the Biological Species Concept, conspecificity (Mashkaryan *et al.*, 2013). Mitochondrial lineages within the *T. graeca* complex correspond to the currently recognized subspecies and have allopatric or parapatric distributions with admixed populations along contact zones (Fritz *et al.*, 2007, 2009; Mashkaryan *et al.*, 2013; Mikulíček *et al.*, 2013). The highest genetic diversity is found in Transcaucasia (Southern Caucasus), which is considered to be the radiation centre of these tortoises (Fritz *et al.*, 2007, 2009). In this region the mitochondrial lineages A (corresponding to *T. g. armeniaca*), C (*T. g. ibera*) and D (*T. g. terrestris*) occur in close proximity. Lineage A is restricted to Transcaucasia and adjacent regions, while lineages C and D have distinctly wider ranges, spreading towards the Balkans and the Middle East, respectively. The genetically diverse lineage B is distributed in north-western Africa and lineages E (*T. g. buxtoni*) and F (*T. g. zarudnyi*) are endemic to western and eastern Iran, respectively. While western Mediterranean populations of the spur-thighed tortoise have been intensively studied over the past years (e.g. Fritz *et al.*, 2009; Vamberger *et al.*, 2011; Anadón *et al.*, 2015), genetic diversity, phylogeography and range dynamics in the easternmost part of the range, and especially in Iran, is poorly known.

In the present study we will focus on exactly this region, using an approach combining detailed phylogeographical data with *N*-dimensional hypervolumes (Blonder *et al.*, 2014), the latter a multivariate technique following the Grinnellian niche concept (Hutchinson, 1957; Soberón & Peterson, 2005; Soberón, 2007). In particular, we aim to (1) assess the present geographical distribution and mitochondrial diversity of the three subspecies of *T. graeca* (*T. g. armeniaca*, *T. g. buxtoni*, *T. g. zarudnyi*) from Iran and Transcaucasia using extensive sampling and the phylogeographically informative mitochondrial cytochrome *b* gene and (2) determine past range dynamics by reconstructing potential distributions for the climatic conditions of the mid-Holocene and the Last Glacial Maximum (LGM).

MATERIAL AND METHODS

Sampling and laboratory procedures

A tally of 64 *T. graeca* from 24 localities (one to four individuals per locality) was sampled between June 2011 and September 2013 in Iran (Table 1, see also Supporting Information, Table S1). A blood sample of each individual was collected from the dorsal coccygeal vein using fine insulin syringes and preserved in 96% ethanol.

DNA was isolated using the NucleoSpin Tissue kit (Macherey-Nagel, Düren, Germany) according to the manufacturer's protocol. We amplified an 1150-bp-long DNA fragment comprising the mitochondrial cytochrome *b* (cyt *b*) gene. The primers mt-A1 (5′-CCCCCTACCAACATCTCAGCAT GATGAAACTTC G-3′) and mtf-na (5′-AGGGTGGAGT CTTCAGTTTTTGGTTTACAAGACCAATG-3′) were used for amplification (Fritz *et al.*, 2007). Polymerase chain reactions (PCRs) were carried out in a 15-μL volume, including 0.7 μl of each PCR primer (10 μM), 7.5 μL of Combi PPP Master Mix (Top-Bio, Prague, Czech Republic), 4.1 μL of PCR water and 2 μL of extracted DNA. After 5 min of initial denaturation at 94 °C followed 35 cycles of 45 s at 94 °C, 52 s at 55 °C

Table 1. Iranian localities of *Testudo graeca* sampled in this study and studies of Fritz *et al.* (2007), Parham *et al.* (2012) and Mashkaryan *et al.* (2013); mitochondrial (mtDNA) lineages were named according to Fritz *et al.* (2007)

Locality	N	E	mtDNA lineage	Reference	No. in Figure 1
Anjir Avand	32.50036	54.43359	F	Fritz *et al.* (2007)	31
Baft	29.22728	56.60382	F	this study	4
Neyriz	29.20125	54.32296	F	Fritz *et al.* (2007)	32
Nir	31.50118	54.13867	F	Fritz *et al.* (2007), this study	33
Rabor	29.28916	56.91308	F	this study	34
Saghand	32.55032	55.22148	F	Fritz *et al.* (2007)	35
Shahr-e Babak	30.11882	55.11837	F	Fritz *et al.* (2007)	36
Tabas	33.59040	56.93741	F	Fritz *et al.* (2007)	37
Kuh-e Taftan	28.60863	61.13330	F	Parham *et al.* (2012)	38
Jolfa	38.87565	45.63222	A	this study	8
Aghchay	38.83333	44.85000	A	this study	39
Aliabad	33.66667	46.56667	E	this study	1
Germi	38.88391	48.01279	E	Fritz *et al.* (2007)	2
Arsanjan	29.91926	53.29770	E	this study	3
Dehlili	34.83333	46.55000	E	this study	5
Divandareh	35.88272	47.01973	E	this study	6
Harzevil	36.73917	49.42946	E	Parham *et al.* (2012)	7
Jolfa	38.87565	45.63222	E	this study	8
Kaleji	38.40000	46.86667	E	this study	9
Khomain	33.66667	49.86667	E	this study	10
Kordabad	32.80000	52.41667	E	this study	11
Kuhpayeh	32.71733	52.43656	E	Fritz *et al.* (2007)	12
Lalabad	34.56667	46.90000	E	Parham *et al.* (2012)	13
Mahidasht	34.25000	46.76667	E	this study	14
Nowshar (Manjil)	36.73559	49.41816	E	Fritz *et al.* (2007)	15
Meshgin Shahr	38.26	47.42	E	Fritz *et al.* (2007)	16
Nazarabad	34.61667	47.51667	E	this study	17
Saravan/Rostamabad	36.57	49.33	E	Fritz *et al.* (2007)	18
Sefid Rud	37.22	48.08	E	Fritz *et al.* (2007)	19
Sepidan	30.20066	51.98653	E	this study	20
Shahrekord	32.35000	50.36667	E	this study	21
Sultanabad	37.31667	45.25000	E	this study	22
Islamabad	34.26667	46.26667	E	this study	23
Ahar	38.76667	46.86667	E	this study	24
Niyaz	38.38333	47.91667	E	this study	25
Siyahdare	34.76667	47.23333	E	this study	26
Kuzerash	38.18333	45.41000	E	this study	27
Nahoj	32.91667	52.63333	E	this study	28
East Azerbaijan Province	37.54	46.16	E	Mashkaryan *et al.* (2013)	29
Zanjan	36.70	48.29	E	Mashkaryan *et al.* (2013)	30

and 80 s at 72 °C, with a final elongation step of 10 min at 72 °C. PCR products were visualized under UV light on a 2% agarose gel with GoldView (SBS Genetech, Beijing, China) and sequenced by the service laboratory Macrogen (Amsterdam, Netherlands). After sequence editing, a 993-bp-long cyt *b* fragment from an originally 1150-bp-long amplicon was used for genetic analysis in 48 individuals. Sequences of 16 individuals (out of the total number of 64) were too short and thus were used only for inferring the distribution pattern of mitochondrial lineages. Sequences are deposited in GenBank (https://www.ncbi.nlm.nih.gov) under accession numbers KY392819–KY392866.

Data analysis

To assign individual haplotypes to the main mitochondrial lineages corresponding to subspecies of *T. graeca*, we computed phylogenetic trees using 993-bp-long cyt *b* sequences generated for this study and sequences

obtained from GenBank (37 cyt *b* sequences from the subspecies *T. g. armeniaca*, *T. g. buxtoni* and *T. g. zarudnyi*, plus sequences from other *T. graeca* subspecies). GenBank sequences of *T. kleinmanni* and *T. marginata* were used as outgroups. Sequences were assembled in SEQMAN 5.05 (DNAStar, Madison, WI, USA) and aligned in BioEdit (Hall, 1999) using the CLUSTALW algorithm (Thompson, Higgins & Gibson, 1994). Data were analysed using Bayesian inference of phylogeny as implemented in MRBAYES 3.1.2. (Ronquist & Huelsenbeck, 2003) for 10^7 generations. Chain convergence and burn-in were estimated according to the indices implemented in MRBAYES (deviation of split frequencies, potential scale reduction factor) and using the program TRACER 1.6 (Rambaut *et al.*, 2013). A consensus tree was constructed using a burn-in of one per 10 000 trees. In addition, a maximum likelihood (ML) analysis was performed using PHYML 2.4.4. (Guindon & Gascuel, 2003). The best evolutionary model was selected with JMODELTEST 0.1.1 (Posada, 2008) using the Akaike information criterion (AIC), resulting in the TPM1UF+G model. Parameters were estimated from the data and a starting tree was obtained via BIONJ. Bootstrap values were calculated using 1000 replicates. FIGTREE 1.4.2 (Rambaut, 2012) was applied for visualizing results.

Uncorrected *p*-distances between the main lineages (subspecies) were calculated using DNASP 5.10.0 (Librado & Rozas, 2009). Genetic diversity within the lineages was estimated as the number of haplotypes (h), haplotype diversity (H_d) and nucleotide diversity (π). Intrasubspecific divergence was estimated and visualized using a 95% statistical parsimony haplotype network built up in the program TCS 1.2.1 (Clement, Posada & Crandall, 2000). This approach is more effective for the presentation of intraspecific evolution than tree-based phylogenies (Posada & Crandall, 2001).

The past population dynamics of the lineages were inferred using the Bayesian coalescent-based approach of the Bayesian skyline plots (BSPs; Drummond *et al.*, 2005) as implemented in BEAST 2.1 (Bouckaert *et al.*, 2014). This analysis estimates the effective population size through time and does not require a specific a priori assumed demographic model (Drummond *et al.*, 2005). Preliminary analyses were run using both a strict molecular clock and an uncorrelated lognormal relaxed molecular clock. Since the parameter of the standard deviation of the uncorrelated lognormal relaxed clock was close to zero, final analyses were run enforcing a strict molecular clock model. A uniform prior for the substitution rate with the initial value 0.0099 substitutions per site per lineage Myr^{-1} (as suggested for the used mtDNA marker in *T. graeca*; Fritz *et al.*, 2009) was set as no internal calibration point was available. The HKY substitution model was selected as the best-fit model by JMODELTEST 2.1 (Darriba *et al.*, 2012). The analyses were run repeatedly to check for consistency between the runs, each for at least ten million generations and sampled every 1000 generations (or more to save 10 000 samples). Convergence, effective sample size (ESS), stationarity and the appropriate number of generations to be discarded as burn-in (10%) were assessed using TRACER 1.6 (Rambaut *et al.*, 2013). The resulting BSPs were also summarized in TRACER 1.6 with the maximum times as the median of the root height parameter.

In addition, the mismatch distributions (MDs) were calculated as the distributions of the observed pairwise nucleotide differences and the expected values under a growing- or declining-population model using DNASP 5.10 (Librado & Rozas, 2009). The principle behind the MDs is that a demographically stable population presents a multimodal (i.e. ragged) distribution of the pairwise nucleotide differences (Slatkin & Hudson, 1991), which will largely deviate from the smooth unimodal distribution found after a demographic expansion. The smoothness of the observed pairwise differences distribution was evaluated by the raggedness statistics (r; Harpending, 1994) with 10 000 coalescent simulations. Finally, the occurrence of historical demographic changes was also assessed by the neutrality-test statistics of Fu's F_S (Fu, 1997), Tajima's D (Tajima, 1989) and Ramos-Onsins and Rozas's R_2 (Ramos-Onsins & Rozas, 2002) calculated in DNASP 5.10 with estimation of the statistical significance using 10 000 coalescent simulations.

Reconstruction of current and historical potential distributions

To determine the present and past potential distributions of *T. graeca* and the respective lineages corresponding to *T. g. buxtoni*, *T. g. zarudnyi* and *T. g. armeniaca* a total of 649 georeferenced occurrence records, constituting all genetic lineages, were obtained from own field research (24) and supplemented with 43 records obtained from scientific publications (Fritz *et al.*, 2007; Parham *et al.*, 2012; Mashkaryan *et al.*, 2013) and 582 records from online databases (GBIF, Vertnet). For current conditions, bioclimatic variables with a spatial resolution of 2.5 arc min (approx. ~5 km at the equator), comprising minima, maxima and mean values of monthly, quarterly and annual ambient temperature as well as precipitation, were obtained from WorldClim (www.worldclim.org) (Hijmans *et al.*, 2005). To assess the impacts of historical climate fluctuations on the distribution of *T. graeca*, we obtained three scenarios for the mid-Holocene (6000 BP) and LGM (21 000 BP) derived from global circulation models (GCMs) through the WorldClim database. These scenarios, namely the Community Climate System Model (CCSM4), the Model for Interdisciplinary Research on

Climate (MIROC-ESM) and the Max-Planck-Institute Earth System Model P (MPI-ESM-P), were statistically down-scaled to a spatial resolution of 2.5 arc min.

We applied an *N*-dimensional hypervolume approach to reconstruct historical niche occupancy of *T. graeca* and the respective lineages E (*T. g. buxtoni*), F (*T. g. zarudnyi*) and A (*T. g. armeniaca*) (Blonder *et al.*, 2014). As environmental background we defined a circular buffer of 200 km enclosing the respective occurrence records. To estimate the environmental space available to each lineage, 10 000 random points were generated across the background and predictor values were extracted from all climate layers including current and past climate information to cover the full correlation structure. As the hypervolume analysis requires orthogonal predictors, we performed a principal component analysis (PCA) trained with environmental information encompassing both current and the two palaeoclimatic time slices to eliminate multi-colinearity. All principal components (PCs) with an eigenvalue exceeding 1 were subsequently projected into geographical space. Following Blonder *et al.* (2014) we determined the shape and volume of each lineage's hypervolume using a multivariate kernel density estimation method. Therefore, we applied a minimum convex polytope (*mcp*) approach, using the hypervolume and dismo packages (Blonder *et al.*, 2014; Hijmans *et al.*, 2014) for CRAN R (R Core Team, 2015). For each lineage the total volume, the area intersecting with any of the other lineages' hypervolumes and the Soerensen similarity index were determined. Subsequently, hypervolumes were projected into geographical space to delimit the potential distribution of each lineage.

Although hypervolumes are intentionally designed to characterize the environmental niche of a species irrespective of predictor weighting, the predictive performance of the hypervolume models was determined using the area under the receiver operating characteristic curve (AUC; Swets, 1988), the point-biserial correlation coefficient (COR; Elith *et al.*, 2006) and Cohen's Kappa (Allouche, Tsoar & Kadmon, 2006) using the relevant functions as implemented in the dismo package for CRAN R.

RESULTS

Distribution and genetic diversity of *T. graeca*

Our phylogenetic analyses, based on the fragment of the mitochondrial cytochrome *b* gene, assigned the Iranian samples to three major clades, present in both the Bayesian and ML trees (data not shown). The first clade was composed of individuals from eastern and southern Iran. It corresponds to clade F of Fritz *et al.* (2007) and is to be identified as *T. g. zarudnyi* (Fig. 1). The second clade comprised tortoises from north-western Iran, bordering Armenia, Nakhjavan (Azerbaijan) and Turkey. We referred this clade to *T. g. armeniaca* (clade A of Fritz *et al.* 2007). The third clade included tortoises from western and central Iran and was equivalent to clade E of Fritz *et al.* (2007), corresponding to *T. g. buxtoni* (Fig. 1). *T. g. armeniaca* and *T. g. buxtoni* haplotypes occurred syntopically in locality 8 (Jolfa; Fig. 1).

The highest pairwise sequence divergence was observed between *T. g. armeniaca* and *T. g. buxtoni* (4.2%). The pairwise divergences between *T. g. zarudnyi* and *T. g. buxtoni* and *T. g. armeniaca* corresponded to 2.9 and 3.6%, respectively.

A total of 23 mtDNA haplotypes were observed. Most diverse was *T. g. buxtoni*, with 13 haplotypes and high values of genetic diversity (Table 2). In the parsimony network analysis, the haplotypes of the three subspecies were not connected, resulting in three distinct networks. The network for *T. g. buxtoni* showed clear geographical structuring with three haplotype clusters, separated by five to seven mutation steps (Fig. 2, see also Supporting Information, Fig. S1). The first two clusters comprised sequences from localities mainly in the Zagros Mountains, while the third cluster corresponded to localities in north-west Iran. Haplotypes from two groups occurred syntopically in localities 17, 18 and 21 (Figs 1, 2). Compared to *T. g. buxtoni*, *T. g. zarudnyi* was less variable with only four different haplotypes (Table 2). Two groups with two haplotypes each were only slightly divergent and distributed mainly in central and eastern Iran, respectively, with a sympatric occurrence in the Hazaran Massif (Kerman province; Fig. 2). The haplotype network of *T. g. armeniaca* was composed of six haplotypes, of which only one extends to Iran (Fig. 2).

Historical demography

BSPs and the complementary MDs for the three subspecies of *T. graeca* are shown in Figure 3. For *T. g. buxtoni* (lineage E) a stable population size was revealed on a long-term scale, followed by a slight recent contraction. The time to most recent common ancestor (TMRCA) value was high (around 600 kya), indicating deep coalescence of lineages and suggestive of the conservation of ancestral genetic variability. In contrast, *T. g. armeniaca* (lineage A) and *T. g. zarudnyi* (lineage F) showed a shallow history with a TMRCA around 250 and 125 kya, respectively. For both subspecies the BSPs profiles suggest moderate demographic increase, particularly during the last 50 kyr. MDs corroborated the results of the BSPs and showed a ragged distribution of the observed values of pairwise differences mainly for *T. g. buxtoni*. In the other two subspecies,

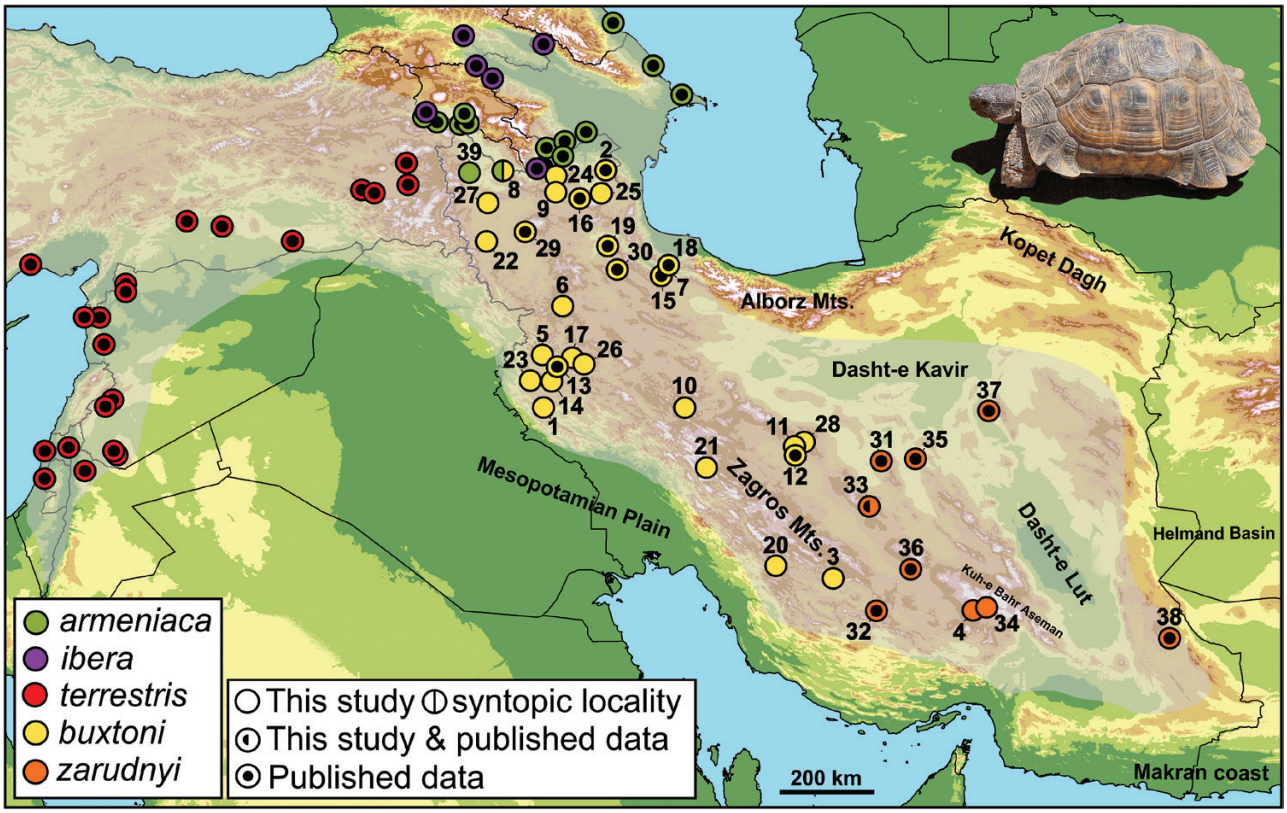

Figure 1. Distribution of the *Testudo graeca* subspecies in Iran and adjacent countries.

Table 2. Genetic diversity within the *Testudo graeca* subspecies estimated as the number of haplotypes (h), nucleotide diversity (π) and haplotype diversity (H_d) and results of historical demographic changes estimated as Fu's F_S, Tajima's D, Ramos-Onsins and Rozas's R_2, and raggedness r statistics. N, number of analysed individuals; $P(F_S)$, $P(D)$, $P(R_2)$, $P(r)$, P-values of the statistical tests

Subspecies	N	h	π (mean ± SD) (%)	H_d (mean ± SD)	F_S	$P(F_S)$	R_2	$P(R_2)$	D	$P(D)$	r	$P(r)$
T. g. armeniaca	25	6	0.26 ± 0.04	0.67 ± 0.07	0.86	0.69	0.11	0.31	0.66	0.28	0.34	0.93
T. g. buxtoni	44	13	0.81 ± 0.06	0.84 ± 0.03	1.75	0.78	0.15	0.90	1.17	0.90	0.04	0.66
T. g. zarudnyi	15	4	0.13 ± 0.02	0.66 ± 0.08	0.31	0.59	0.16	0.46	0.27	0.65	0.21	0.60

distributions were less ragged, although none of the observed values supported a growing- or declining-population model. The raggedness statistics as well as the neutrality tests did not show statistically significant population expansions (Table 2).

Species distribution modelling

The PCA revealed three PCs with eigenvalues exceeding 1; the contribution of each environmental predictor variable to each PC is specified in Table 3. The first two PCs with eigenvalues of 10.41 and 3.89, respectively, explained 55 and 20% of the total variation while PC3 had an eigenvalue of 1.82 and explained 9.56% of the total variation (see Supporting Information, Fig. S2). Variable contribution to the first PC was highest in 'annual precipitation' (Bio 12), followed by 'precipitation of the driest, warmest and wettest quarter' (Bio 17, Bio 18, Bio 16). The second PC mainly correlates to 'temperature seasonality' (Bio 4) and 'temperature annual range' (Bio 7), while the third PC refers to 'precipitation seasonality' (Bio 15), 'precipitation of the coldest quarter' (Bio 19) and 'mean temperature of the driest quarter' (Bio 9) (Table 3).

Model performance for the three-dimensional hypervolumes of *T. g. buxtoni*, *T. g. zarudnyi* and *T. g. armeniaca* ranged between 0.57 and 0.60 in AUC, 0.04 and 0.15 in COR, and 0.02 and 0.14 in Kappa (Table 4). The

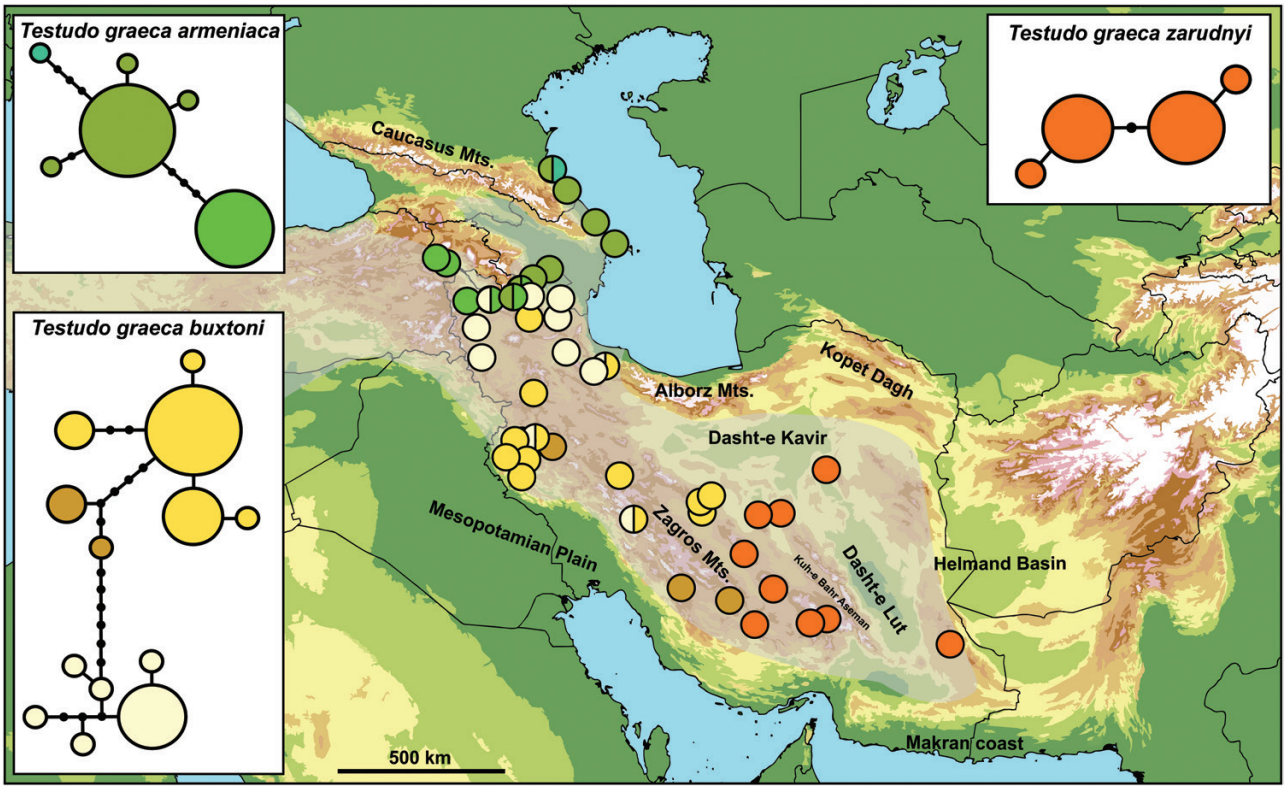

Figure 2. Distribution and genetic differentiation of *Testudo graeca armeniaca*, *Testudo graeca buxtoni* and *Testudo graeca zarudnyi*, and 95% statistical parsimony haplotype networks based on the mitochondrial cytochrome *b* fragment. The sizes of the circles in the haplotype networks are proportional to the haplotype frequencies.

largest total volume by far was obtained for *T. g. buxtoni*, while the hypervolumes for *T. g. armeniaca* and *T. g. zarudnyi* were significantly smaller (Table 4).

There was only a small intersecting area (overlap between hypervolumes in PC space) between *T. g. buxtoni* and *T. g. zarudnyi* (2.06), and *T. g. buxtoni* and *T. g. armeniaca* (0.11) and no overlap between the lineages *T. g. armeniaca* and *T. g. zarudnyi* (0.00) (Table 5). Concordantly, the Soerensen similarity index between pairs of lineages was small in the neighbouring subspecies *T. g. buxtoni* and *T. g. zarudnyi* (0.15), and *T. g. armeniaca* and *T. g. buxtoni* (0.01), while there was no overlap between the geographically more distant lineages *T. g. armeniaca* and *T. g. zarudnyi* (Table 5).

The present potential distributions derived from the respective hypervolume models are generally in line with the known distribution ranges (Figs. 4–6; see also Supporting Information, Fig. S3). However, while the potential distribution for *T. g. armeniaca* matches completely with its actual distribution, the models suggest additional environmentally suitable space to stretch eastwards into Afghanistan and westwards into Iraq for *T. g. zarudnyi*. Similarly, for *T. g. buxtoni* environmentally suitable conditions are predicted in Afghanistan and Turkey.

While for *T. g. armeniaca* suitable space has been relatively stable since the LGM, projections onto palaeoclimatic conditions concordantly predict potentially suitable space for *T. g. buxtoni* and *T. g. zarudnyi* to have contracted rather than expanded since then (Figs 4–6).

DISCUSSION

Prior to our study, the distribution ranges of the subspecies of *T. graeca* were unclear in many parts of Iran, in particular in the central regions of the country, where the ranges of *T. g. buxtoni* and *T. g. zarudnyi* are expected to abut. Three subspecies, *T. g. armeniaca*, *T. g. buxtoni* and *T. g. zarudnyi*, show a parapatric distribution in Iran, each of which harbours a distinct mitochondrial lineage [lineages A, E and F sensu Fritz *et al.* (2007), respectively]. *T. g. armeniaca* was recorded for the first time for Iran in the present study, being confined only to the north-westernmost part of the country, from where the range extends into eastern Turkey, Armenia, Azerbaijan and Dagestan (Fritz *et al.*, 2007; Mashkaryan *et al.*, 2013). *T. g. buxtoni* is most widely distributed and occurs from north-western to central Iran, while *T. g. zarudnyi* occupies central and eastern Iran. Two further subspecies known

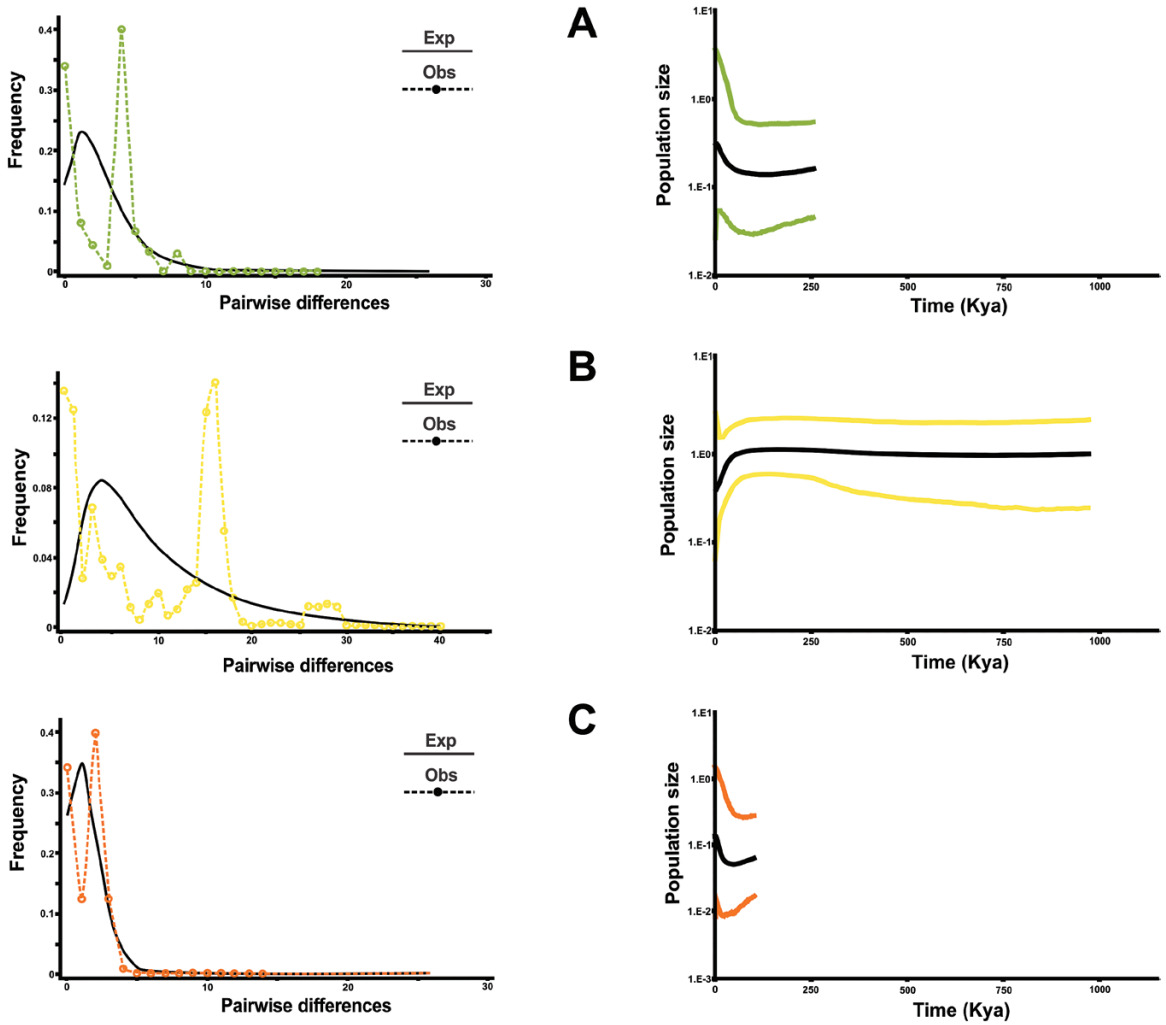

Figure 3. Mismatch distributions (MDs) and Bayesian skyline plots (BSPs) based on the cytochrome *b* fragment for *Testudo graeca armeniaca* (A), *Testudo graeca buxtoni* (B) and *Testudo graeca zarudnyi* (C). The dotted lines in the MDs show the frequency distribution of the observed pairwise differences; the solid lines show the frequency distribution of the expected pairwise differences under the expansion model. In BSPs, the *x*-axis shows time before present in years, and the *y*-axis shows the effective population size. Coloured lines in BSPs show the 95% high posterior density of the effective population size through time.

from the Caucasus region and Turkey (*T. g. ibera* and *T. g. terrestris*) were not recorded in Iran, despite their occurrence in southern Armenia (Mashkaryan *et al.*, 2013) and the easternmost part of Turkey (Fritz *et al.*, 2007), respectively.

Since we only used a mitochondrial marker for subspecies identification and assignment based on morphological features in this highly variable species is considered impossible (Fritz *et al.*, 2007), we cannot exclude that the subspecies ranges as outlined in the present study are compromised by mitochondrial introgression. However, two previous studies combined nuclear markers (AFLPs, Mikulíček *et al.* 2013; microsatellites, Mashkaryan *et al.*, 2013) with mtDNA and found only very limited evidence for mitochondrial introgression, even though the subspecies of *T. graeca* hybridize massively in Transcaucasia (Mashkaryan *et al.*, 2013). According to these studies, introgression of mtDNA is restricted to the narrow hybrid zones. Thus, we are confident that our range delimitation using mitochondrial data is an appropriate approach and that our inferences on range dynamics are sound.

Precipitation was revealed as the main restricting parameter shaping the distribution of *T. graeca* in Iran and Transcaucasia. Concordantly, also in the western Mediterranean rainfall was the most limiting factor for the distribution of this species (Anadón *et al.*, 2012, 2015). Precipitation influences primary

Table 3. Principal component summary including Pearson product correlation coefficients, Eigenvalues and explained total variance; highest values are displayed in bold type

Abbreviation	Variable	PC 1	PC 2	PC 3
Bio 1	Annual mean temperature	–0.88	–0.41	–0.07
Bio 2	Mean annual range (mean of monthly (T max – T min))	–0.8	0.1	0.08
Bio 3	Isothermality (Bio 2 / Bio 7) × 100	–0.61	–0.6	0.01
Bio 4	Temperature seasonality (SD × 100)	0.01	0.94	0.05
Bio 5	Max T of warmest month	–0.93	0.06	0.02
Bio 6	Min T of coldest month	–0.6	–0.77	–0.06
Bio 7	T annual range (Bio 5 – Bio 6)	–0.34	0.87	0.08
Bio 8	Mean T of wettest quarter	–0.44	–0.28	–0.63
Bio 9	Mean T of driest quarter	–0.71	–0.12	0.49
Bio 10	Mean T of warmest quarter	–0.92	–0.04	–0.04
Bio 11	Mean T of coldest quarter	–0.73	–0.67	–0.06
Bio 12	Annual precipitation	0.91	–0.3	0.15
Bio 13	Precipitation of wettest month	0.82	–0.32	0.37
Bio 14	Precipitation of driest month	0.85	–0.21	–0.31
Bio 15	Precipitation seasonality (CV)	–0.55	–0.17	0.57
Bio 16	Precipitation of wettest quarter	0.83	–0.32	0.36
Bio 17	Precipitation of driest quarter	0.87	–0.23	–0.27
Bio 18	Precipitation of warmest quarter	0.85	–0.19	–0.34
Bio 19	Precipitation of coldest quarter	0.72	–0.35	0.50
Eigenvalue		10.41	3.89	1.82
Explained variance		54.81	20.45	9.56

Table 4. Test statistics and total volume of hypervolumes for the *Testudo graeca* subspecies

Subspecies	Volume	AUC	COR	Kappa
T. g. armeniaca	2.94	0.60	0.15	0.14
T. g. buxtoni	21.92	0.60	0.10	0.07
T. g. zarudnyi	4.68	0.57	0.04	0.02

Table 5. Intersection area (italics) and Soerensen overlap (bold) for the *Testudo graeca* subspecies. Soerensen indices range from 0 (no overlap) to 1 (niches are identical): S = 2 × intersection/(unique Volume *x* + unique Volume *y*)

Subspecies	*T. g. armeniaca*	*T. g. buxtoni*	*T. g. zarudnyi*
T. g. armeniaca		**0.01**	**0.00**
T. g. buxtoni	*0.11*		**0.16**
T. g. zarudnyi	*0.00*	*2.09*	

productivity in ecosystems and thus affects tortoise survival. Extensive deserts such as the Dasht-e Kavir and the Dasht-e Lut in Iran are characterized by an extremely arid climate and therefore represent crucial biogeographical barriers limiting the distribution of *T. graeca*. Other environmental variables shaping the distribution of tortoises in Iran and Transcaucasia are the seasonal variation in temperature expressed as 'temperature seasonality' and 'annual temperature range'. Seasonal temperature variation seems to be a limiting factor for tortoises in the Middle East, since this region is characterized by a continental climate with hot summers and cold winters. Hence, the combination of precipitation and high temperature seasonality appear to shape the distributional pattern of *T. graeca* in the eastern part of its range.

A comparison of the current distribution patterns and the reconstructed historical ranges of *T. graeca* reveals that the distribution ranges of the three subspecies in Iran and Transcaucasia have not changed substantially since the LGM (*c.* 21 000 BP; Figs 4–6). This contrasts with the general pattern for many species in high latitudes, which typically retreated to refugia in the southern European peninsulas, Asia Minor or in the Ponto-Caspian region, and expanded their ranges substantially in the Holocene (Taberlet *et al.*, 1998; Hewitt, 2000; Schmitt, 2007; Stewart *et al.*, 2010; but see, for example, Stewart & Lister, 2001; Vörös *et al.*, 2016). The palaeomodels suggest that the studied *T. graeca* subspecies reveal relative stability or only slight shifts/contractions of their ranges since the LGM. The tortoises did not retreat to glacial refugia, defined as significantly contracted geographical regions that a species inhabits during a glacial cycle (Stewart *et al.*, 2010). It even seems that specifically *T. g. buxtoni* occupied a larger

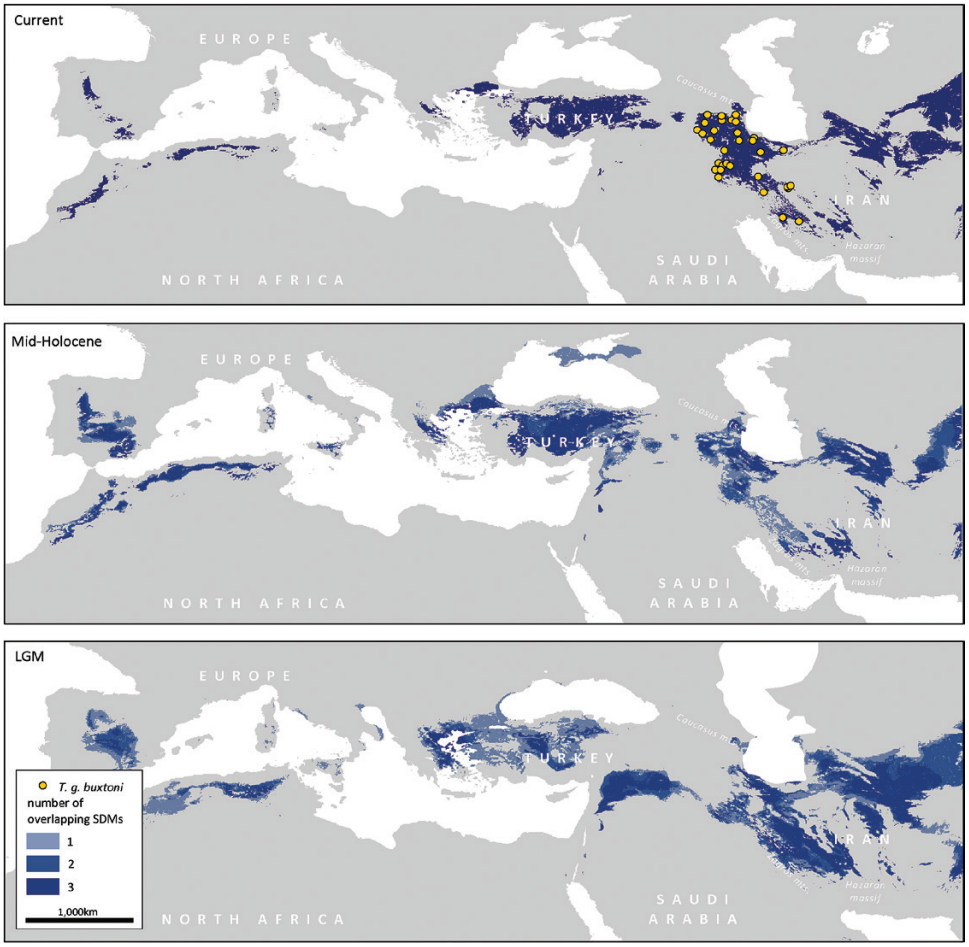

Figure 4. Three-dimensional hypervolumes of the environmental niches for *Testudo graeca buxtoni.* Circles represent georeferenced occurrence records obtained from our own field research, scientific publications (Fritz *et al.*, 2007; Parham *et al.*, 2012; Mashkaryan *et al.*, 2013) and online databases (GBIF, Vertnet).

distribution range during the LGM, which slightly contracted during the mid-Holocene. Palaeoecological and palynological studies suggest that in comparison to the Holocene, the LGM in Iran was characterized by a cooler and more arid climate, which was associated with an expansion of grass steppes (Ray & Adams, 2001; Djamali *et al.*, 2008, 2011, 2012; Kehl, 2009). High tolerance of *T. graeca* to a wide range of climatic conditions together with widespread grassland habitats might have allowed the survival and promoted a vast geographical distribution of tortoises even during the LGM. Several estimates show that average temperature during the LGM in different parts of Iran was 5–10 °C lower than today (see Kehl, 2009, and references therein). These differences resemble the variation in average annual temperature in various parts of the extant range of *T. graeca*, including Iran (e.g. the difference in average annual temperature of Yazd in central Iran and Ardabil in north-western Iran is 5.3 °C). Similarly, there are significant differences within the range of *T. graeca* in precipitation, with some populations living in areas with rainfall values of 800–1200 mm (north-western Africa; Anadón *et al.*, 2015) and others inhabiting arid conditions in the Iranian semideserts, where average annual precipitation does not exceed 100 mm. These facts show that *T. graeca* is an ecologically plastic species and is able to adapt to a wide range of different environments. High ecological plasticity could have been one reason for the relative stability of the distribution ranges of the *T. graeca* subspecies in Iran and Transcaucasia since the LGM. This biogeographical pattern contrasts with some plant, butterfly and lizard species in Iran, which either experienced range contractions to glacial refugia in the Zagros Mountains, the Lesser Caucasus and the Alborz Mountains (Ahmadzadeh *et al.*, 2013; Rajaei Sh *et al.*, 2013) or, in the case of psychrophilic species, retreated during interglacials to so-called interglacial

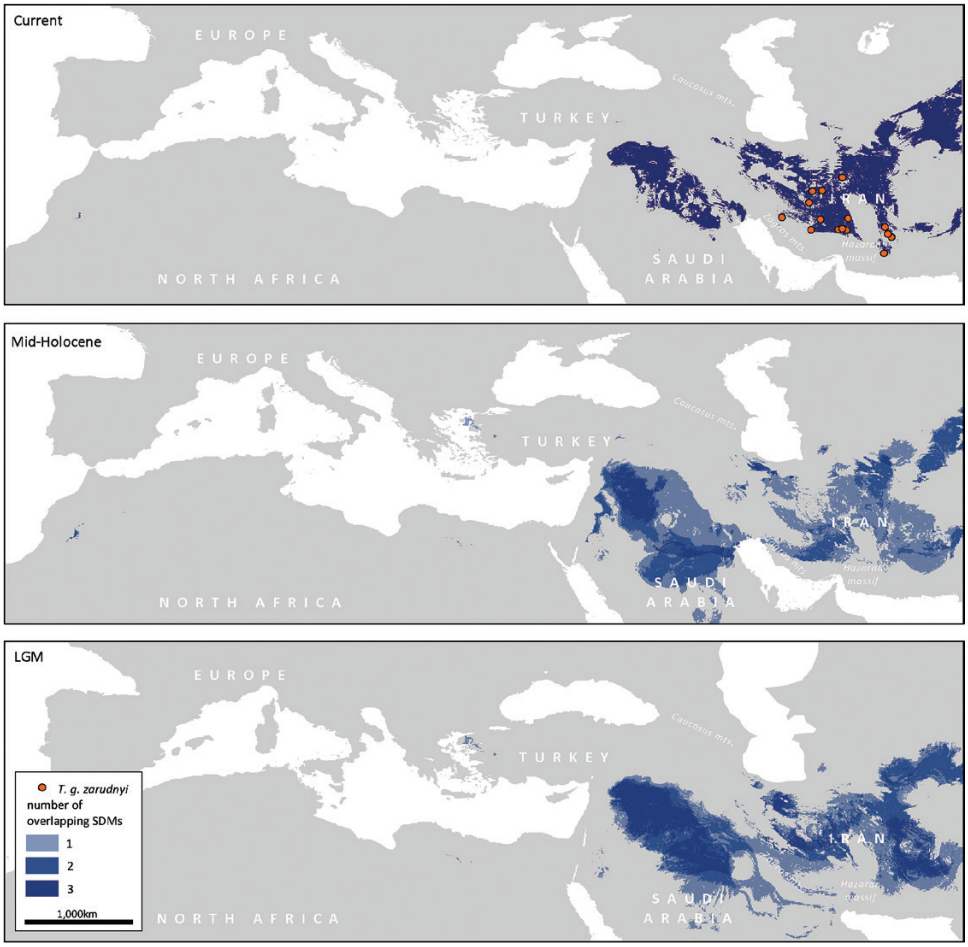

Figure 5. Three-dimensional hypervolumes of the environmental niches for *Testudo graeca zarudnyi*. Circles represent georeferenced occurrence records obtained from our own field research, scientific publications (Fritz *et al.*, 2007; Parham *et al.*, 2012; Mashkaryan *et al.*, 2013) and online databases (GBIF, Vertnet).

refugia (Djamali *et al.*, 2012). However, the ranges of two eastern Mediterranean and Middle Eastern terrapin species (*Mauremys caspica*, *M. rivulata*) also have shifted only little since the LGM (Vamberger *et al.*, 2016), suggesting that the pattern revealed for *T. graeca* may be not unique and that further ectothermic species from the Middle East should be examined to elucidate these unexpected patterns in more detail.

Our results of the species distribution models agree with our demographic analyses, which do not corroborate the hypothesis of postglacial population expansions for the subspecies of *T. graeca*, in contrast to many western Palaearctic species that expanded their ranges from local glacial refugia (including species distributed in Iran; Ahmadzadeh *et al.*, 2013; Rajaei Sh *et al.*, 2013). Long-term survival of *T. graeca* populations in situ led to high genetic diversity. Among the studied subspecies, genetic diversity is highest in the widely distributed subspecies *T. g. buxtoni*, while *T. g. armeniaca* and *T. g. zarudnyi* have smaller ranges and a lower genetic diversity. Moreover, *T. g. buxtoni* is geographically clearly structured with three haplotype groups. The first two groups are distributed mainly across the Zagros Mountains, while the third, more divergent group is restricted to north-western Iran. Haplotypes from two groups co-occur at three localities (see Figs 1, 2). This syntopic occurrence is not straightforward to interpret. One possibility is that this pattern results from secondary contact of both haplogroups. However, it also cannot be excluded that tortoises were translocated by humans (cf. Graciá *et al.*, 2011).

Responses of species to Quaternary climatic changes in lower latitudes are complex and vary between the species with respect to their specific adaptations and environmental tolerance (Stewart *et al.*, 2010). However, Anadón *et al.* (2015) demonstrated that species-specific responses to climatic fluctuations in lower

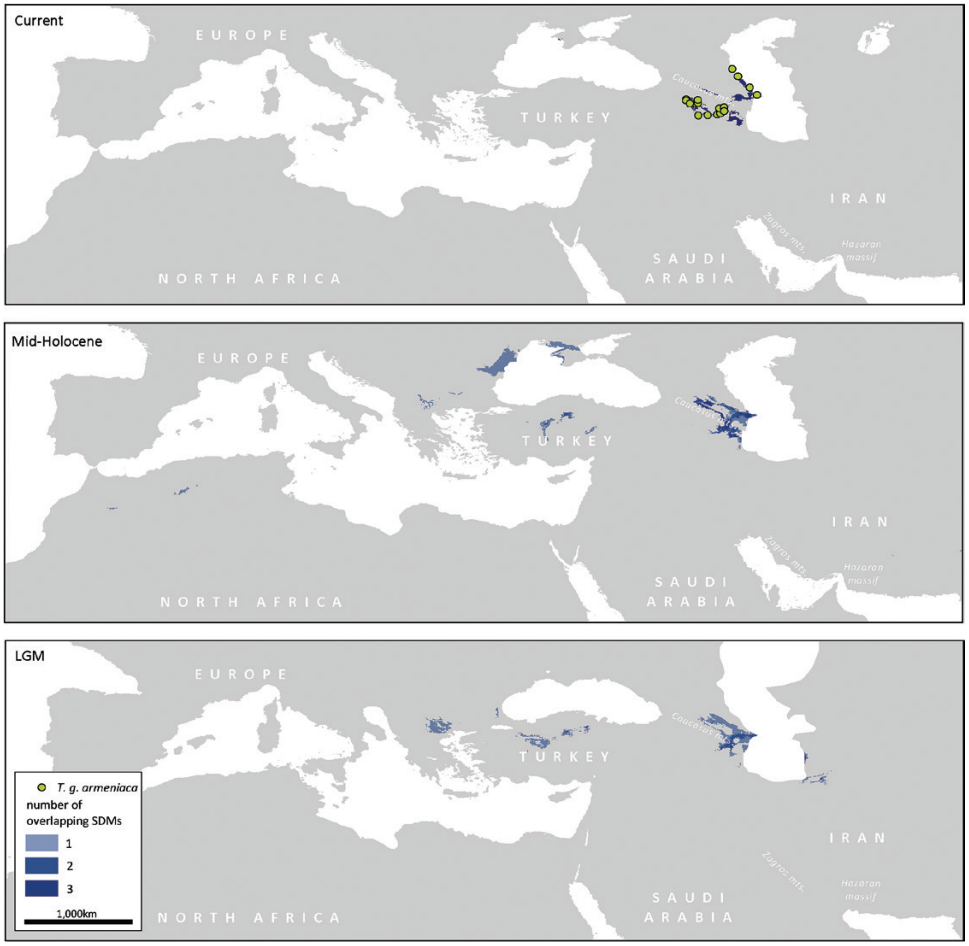

Figure 6. Three-dimensional hypervolumes of the environmental niches for *Testudo graeca armeniaca.* Circles represent georeferenced occurrence records obtained from our own field research, scientific publications (Fritz *et al.*, 2007; Parham *et al.*, 2012; Mashkaryan *et al.*, 2013) and online databases (GBIF, Vertnet).

latitudes are also more unpredictable. This unpredictability might be related to the fact that the distribution of species in lower latitudes is not predominately limited by temperature (like in species from mid- and high latitudes), but also depends on other parameters and a combination of different variables, such as precipitation or complex topography (Anadón *et al.*, 2015). Our study focusing on genetic diversity and distribution of *T. graeca* in Iran and Transcaucasia corroborates that the patterns of Quaternary range dynamics in ectothermic vertebrates cannot follow a simplistic scenario of glacial retraction and postglacial range expansion. Instead, populations of species in lower latitudes might reveal a long-term stability of their ranges resulting in relatively high genetic diversity. Finally, our work contributes to an understanding of the historical biogeography of Iran, which, despite its high species diversity and endemism, remains a biologically poorly known country in the Middle East.

ACKNOWLEDGEMENTS

We thank all colleagues and local people for their help in sampling tortoises in Iran. We also thank two anonymous reviewers for their helpful comments. This work was supported by the Slovak Research and Development Agency under contract No. APVV-0147-15 and by the project Center of excellence for protection and use of landscape and for biodiversity (ITMS: 26240120014).

REFERENCES

Ahmadzadeh F, Carretero MA, Rödder D, Harris DJ, Nunes Freitas S, Perera A, Böhme W. 2013. Inferring the effects of past climate fluctuations on the distribution pattern of *Iranolacerta* (Reptilia, Lacertidae): evidence from mitochondrial DNA and species distribution models. *Zoologischer Anzeiger* **252:** 141–148.

Allouche O, Tsoar A, Kadmon R. 2006. Assessing the accuracy of species distribution models: prevalence, kappa and the true skill statistic (TSS). *Journal of Applied Ecology* **43:** 1223–1232.

Anadón JD, Giménez A, Graciá E, Pérez I, Ferrández M, Fahd S, El Mouden H, Kalboussi M, Jdeidi T, Larbes S, Rouag R, Slimani T, Znari M, Fritz U. 2012. Distribution of *Testudo graeca* in the western Mediterranean according to climatic factors. *Amphibia-Reptilia* **33:** 285–296.

Anadón JD, Graciá E, Botella F, Giménez A, Fahd S, Fritz U. 2015. Individualistic response to past climate changes: niche differentiation promotes diverging Quaternary range dynamics in the subspecies of *Testudo graeca*. *Ecography* **38:** 956–966.

Avise JC. 2000. *Phylogeography: The history and formation of species.* Cambridge, MA: Harvard University Press.

Blonder B, Lamanna C, Violle C, Enquist BJ. 2014. The n-dimensional hypervolume. *Global Ecology and Biogeography* **23:** 595–609.

Bouckaert R, Heled J, Kühnert D, Vaughan T, Wu CH, Xie D, Suchard MA, Rambaut A, Drummond AJ. 2014. BEAST 2: a software platform for Bayesian evolutionary analysis. *PLoS Computational Biology* **10:** e1003537.

Clement M, Posada D, Crandall K. 2000. TCS: a computer program to estimate gene genealogies. *Molecular Ecology* **9:** 1657–1659.

Darriba D, Taboada GL, Doallo R, Posada D. 2012. jModelTest 2: more models, new heuristics and parallel computing. *Nature Methods* **9:** 772.

Djamali M, de Beaulieu J-L, Shah-hosseini M, Andrieu-Ponel V, Ponel P, Amini A, Akhani H, Leroy SAG, Stevens L, Lahijani H, Brewer S. 2008. A late Pleistocene long pollen record from Lake Urmia, NW Iran. *Quaternary Research* **69:** 413–420.

Djamali M, Biglari F, Abdi K, Andrieu-Ponel V, de Beaulieu J-L, Mashkour M, Ponel P. 2011. Pollen analysis of coprolites from a late Pleistocene–Holocene cave deposit (Wezmeh Cave, west Iran): insights into the late Pleistocene and late Holocene vegetation and flora of the central Zagros Mountains. *Journal of Archaeological Science* **38:** 3394–3401.

Djamali M, Baumel A, Brewer S, Jackson ST, Kadereit JW, López-Vinyallonga S, Mehregan I, Shabanian E, Simakova A. 2012. Ecological implications of *Cousinia* Cass. (Asteraceae) persistence through the last two glacial–interglacial cycles in the continental Middle East for the Irano-Turanian flora. *Review of Palaeobotany and Palynology* **172:** 10–20.

Drummond AJ, Rambaut A, Shapiro B, Pybus OG. 2005. Bayesian coalescent inference of past population dynamics from molecular sequences. *Molecular Biology and Evolution* **22:** 1185–1192.

Elith J, Graham CH, Anderson RP, Dudík M, Ferrier S, Guisan A, Hijmans RJ, Huettmann F, Leathwick JR, Lehmann A, Loiselle BA, Manion G, Moritz C, Nakamura M, Nakazawa Y, Overton J McC, Peterson AT, Phillips SJ, Richardson KS, Scachetti-Pereira R, Schapire RE, Soberón J, Williams S, Wisz MS, Zimmermann NE. 2006. Novel methods improve prediction of species' distributions from occurrence data. *Ecography* **29:** 129–151.

Fritz U, Havaš P. 2007. Checklist of Chelonians of the World. *Vertebrate Zoology* **57:** 149–368.

Fritz U, Hundsdörfer AK, Široký P, Auer M, Kami H, Lehman J, Mazaneva LF, Türkozan O, Wink M. 2007. Phenotypic plasticity leads to incongruence between morphology-based taxonomy and genetic differentiation in western Palaearctic tortoises (*Testudo graeca* complex; Testudines, Testudinidae). *Amphibia-Reptilia* **28:** 97–121.

Fritz U, Harris DJ, Fahd S, Rouag R, Graciá Martínez E, Giménez Casalduero A, Široký P, Kalboussi M, Jdeidi TB, Hundsdörfer AK. 2009. Mitochondrial phylogeography of *Testudo graeca* in the Western Mediterranean: old complex divergence in North Africa and recent arrival in Europe. *Amphibia-Reptilia* **30:** 63–80.

Fu Y-X. 1997. Statistical tests of neutrality of mutations against population growth, hitchhiking and background selection. *Genetics* **147:** 913–925.

Graciá E, Giménez A, Anadón JD, Botella F, García-Martínez S, Marín M. 2011. Genetic patterns of a range expansion: the Spur-thighed tortoise *Testudo graeca* graeca in southeastern Spain. *Amphibia-Reptilia* **32:** 49–61.

Guindon S, Gascuel O. 2003. A simple, fast, and accurate algorithm to estimate large phylogenies by maximum likelihood. *Systematic Biology* **52:** 696–704.

Hall TA. 1999. BioEdit: a user-friendly biological sequence alignment editor and analysis program for Windows 95/98/NT. *Nucleic Acids Symposium Series* **41:** 95–98.

Harpending HC. 1994. Signature of ancient population growth in a low-resolution mitochondrial DNA mismatch distribution. *Human Biology* **66:** 591–600.

Hewitt G. 2000. The genetic legacy of the Quaternary ice ages. *Nature* **405:** 907–913.

Hewitt GM. 2011. Quaternary phylogeography: the roots of hybrid zones. *Genetica* **139:** 617–638.

Hijmans RJ, Cameron SE, Parra JL, Jones PG, Jarvis A. 2005. Very high resolution interpolated climate surfaces for global land areas. *International Journal of Climatology* **25:** 1965–1978.

Hijmans RJ, Phillips S, Leathwick J, Elith J. 2014. *Dismo: species distribution modeling. R package version 1.0–5*. Available at: http://CRAN.R-project.org/package=dismo.

Hutchinson G. 1957. Concluding remarks. *Cold Spring Harbor Symposia on Quantitative Biology* **22:** 415–427.

Kehl M. 2009. Quaternary climate change in Iran – the state of knowledge. *Erdkunde* **63:** 1–17.

Librado P, Rozas J. 2009. DnaSP v5: a software for comprehensive analysis of DNA polymorphism data. *Bioinformatics* **25:** 1451–1452.

Mashkaryan V, Vamberger M, Arakelyan M, Hezaveh N, Carretero MA, Corti C, Harris D, Fritz U. 2013. Gene flow among deeply divergent mtDNA lineages of *Testudo graeca* (Linnaeus, 1758) in Transcaucasia. *Amphibia-Reptilia* **34:** 337–351.

Médail F, Diadema K. 2009. Glacial refugia influence plant diversity patterns in the Mediterranean Basin. *Journal of Biogeography* **36:** 1333–1345.

Mikulíček P, Jandzik D, Fritz U, Schneider C, Široký P. 2013. AFLP analysis shows high incongruence between genetic differentiation and morphology-based taxonomy in a widely distributed tortoise. *Biological Journal of the Linnean Society* **108:** 151–160.

Parham JF, Stuart BL, Danilov IG, Ananjeva NB. 2012. A genetic characterization of CITES-listed Iranian tortoises (*Testudo graeca*) through the sequencing of topotypic samples and a 19th century holotype. *Herpetological Journal* **22:** 73–78.

Posada D. 2008. jModelTest: phylogenetic model averaging. *Molecular Biology and Evolution* **25:** 1253–1256.

Posada D, Crandall KA. 2001. Intraspecific gene genealogies: trees grafting into networks. *Trends in Ecology & Evolution* **16:** 37–45.

Rajaei Sh H, Rödder D, Weigand AM, Dambach J, Raupach MJ, Wägele JW. 2013. Quaternary refugia in southwestern Iran: insights from two sympatric moth species (Insecta, Lepidoptera). *Organisms, Diversity and Evolution* **13:** 409–423.

Rambaut A. 2012. *FigTree.* Available at: http://tree.bio.ed.ac.uk/software/figtree/

Rambaut A, Suchard MA, Xie W, Drummond AJ. 2013. *Tracer v1.6.* Available at: http://beast.bio.ed.ac.uk/Tracer

Ramos-Onsins SE, Rozas J. 2002. Statistical properties of new neutrality tests against population growth. *Molecular Biology and Evolution* **19:** 2092–2100.

Ray N, Adams JN 2001. A GIS-based vegetation map of the world at the last glacial maximum (25,000-15,000 BP). *Internet Archaeology* **11**. Available at: http://intarch.ac.uk/journal/issue11/rayadams_toc.html

Ronquist F, Huelsenbeck JP. 2003. MrBayes 3: Bayesian phylogenetic inference under mixed models. *Bioinformatics* **19:** 1572–1574.

Schmitt T. 2007. Molecular biogeography of Europe: Pleistocene cycles and postglacial trends. *Frontiers in Zoology* **4:** 11.

Slatkin M, Hudson RR. 1991. Pairwise comparisons of mitochondrial DNA sequences in stable and exponentially growing populations. *Genetics* **129:** 555–562.

Soberón J. 2007. Grinnellian and Eltonian niches and geographic distributions of species. *Ecology Letters* **10:** 1115–1123.

Soberón J, Peterson T. 2005. Interpretation of models of fundamental ecological niches and species' distributional areas. *Biodiversity Informatics* **2:** 1–10.

Stewart JR, Lister AM. 2001. Cryptic northern refugia and the origin of the modern biota. *Trends in Ecology and Evolution* **16:** 608–613.

Stewart JR, Lister AM, Barnes I, Dalen L. 2010. Refugia revised: individualistic responses of species in space and time. *Proceedings of the Royal Society B* **277:** 661–671.

Swets JA. 1988. Measuring the accuracy of diagnostic systems. *Science* **240:** 1285–1293.

Taberlet P, Fumagalli L, Wust-Saucy AG, Cosson JF. 1998. Comparative phylogeography and postglacial colonization routes in Europe. *Molecular Ecology* **7:** 453–464.

Tajima F. 1989. Statistical method for testing the neutral mutation hypothesis by DNA polymorphism. *Genetics* **123:** 585–595.

Thompson JD, Higgins DG, Gibson TJ. 1994. CLUSTAL W: improving the sensitivity of progressive multiple sequence alignment through sequence weighting, position-specific gap penalties and weight matrix choice. *Nucleic Acids Research* **22:** 4673–4680.

Vamberger M, Corti C, Stuckas H, Fritz U. 2011. Is the imperilled Spur-thighed tortoise (*Testudo graeca*) native in Sardinia? Implications from population genetics and for conservation. *Amphibia-Reptilia* **32:** 9–25.

Vamberger M, Stuckas H, Vargas-Ramírez M, Kehlmaier C, Ayaz D, Aloufi AA, Lymberakis P, Fritz U. 2016. Unexpected hybridization patterns in Near Eastern terrapins (*Mauremys caspica*, *M. rivulata*) indicate ancient gene flow across the Fertile Crescent. *Zoologica Scripta*, doi:10.1111/zsc.12227.

Vörös J, Mikulíček P, Major A, Recuero E, Arntzen JW. 2016. Phylogeographic analysis reveals northerly refugia for the riverine amphibian *Triturus dobrogicus* (Caudata: Salamandridae). *Biological Journal of the Linnean Society* **119:** 974–991.

SUPPORTING INFORMATION

Additional Supporting Information may be found in the online version of this article at the publisher's website:

Figure S1. Parsimony haplotype networks for *Testudo graeca armeniaca*, *Testudo graeca buxtoni* and *Testudo graeca zarudnyi* based on the mitochondrial cytochrome *b* fragment. The sizes of the circles in the haplotype networks are proportional to the haplotype frequencies.

Figure S2. Principal component analysis (PCA) showing the position of the *Testudo graeca* subspecies in environmental space. The points represent the centroid of the respective taxa, while the lines show the 95% confidence intervals.

Figure S3. Three-dimensional hypervolumes of the environmental niches for *Testudo graeca.* Circles represent 650 georeferenced occurrence records of *T. graeca* obtained from our own field research, scientific publications (Fritz *et al.*, 2007; Parham *et al.*, 2012; Mashkaryan *et al.*, 2013) and online databases (GBIF, Vertnet).

Table S1. A list of *Testudo graeca* samples analyzed for cytochrome *b* variation.

Genetic diversity and Quaternary range dynamics in Iranian and Transcaucasian tortoises

Hossein Javanbakht[1], Flora Ihlow[2], Daniel Jablonski[3], Pavel Široký[4], Uwe Fritz[5], Dennis Rödder[2], Mozafar Sharifi[6], Peter Mikulíček[3]

Biological Journal of the Linnean Society, 2017

DOI: https://doi.org/10.1093/biolinnean/blx001

Supporting Information

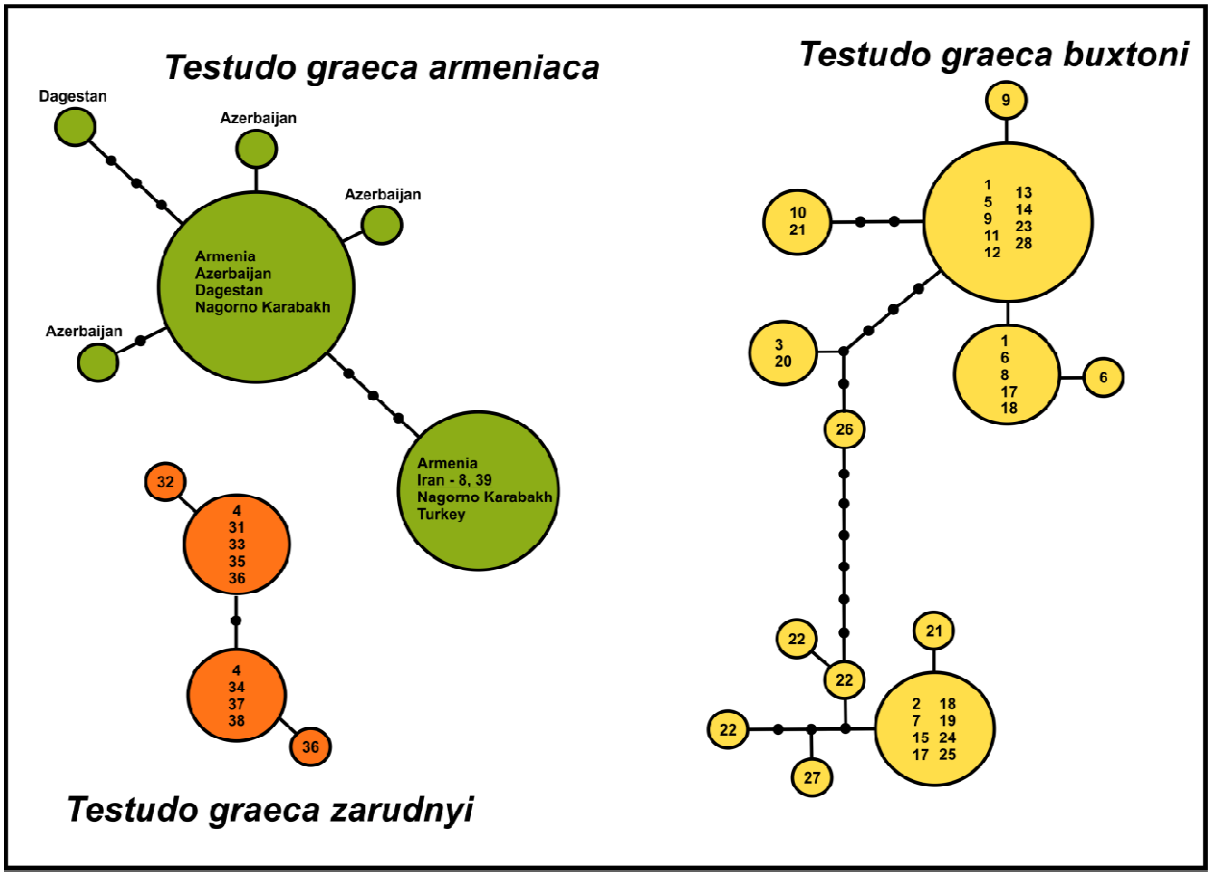

Figure S1 Parsimony haplotype networks for *Testudo graeca armeniaca*, *Testudo graeca buxtoni* and *Testudo graeca zarudnyi* based on the mitochondrial cytochrome *b* fragment. The sizes of the circles in the haplotype networks are proportional to the haplotype frequencies.

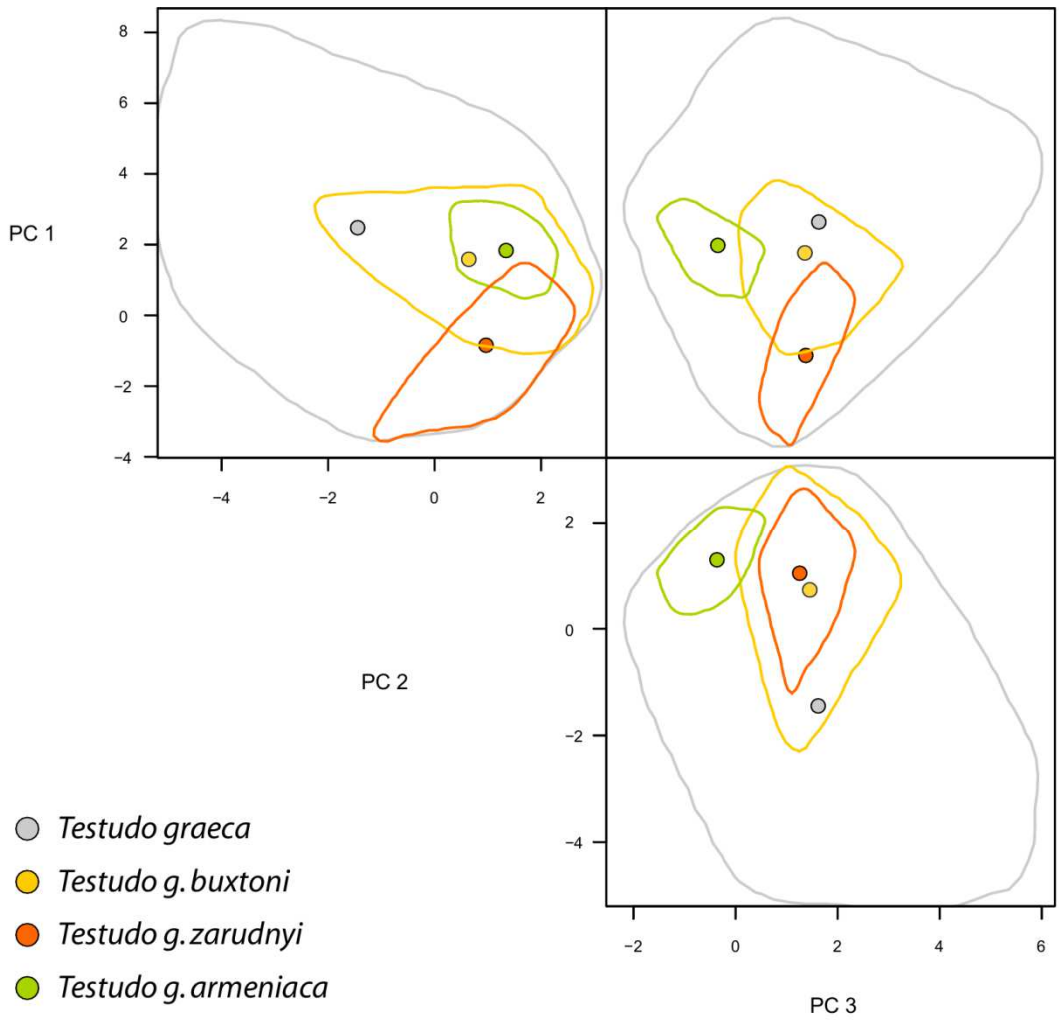

Figure S2 Principal component analysis (PCA) showing the position of the *Testudo graeca* subspecies in environmental space. The points represent the centroid of the respective taxa, while the lines show the 95% confidence intervals.

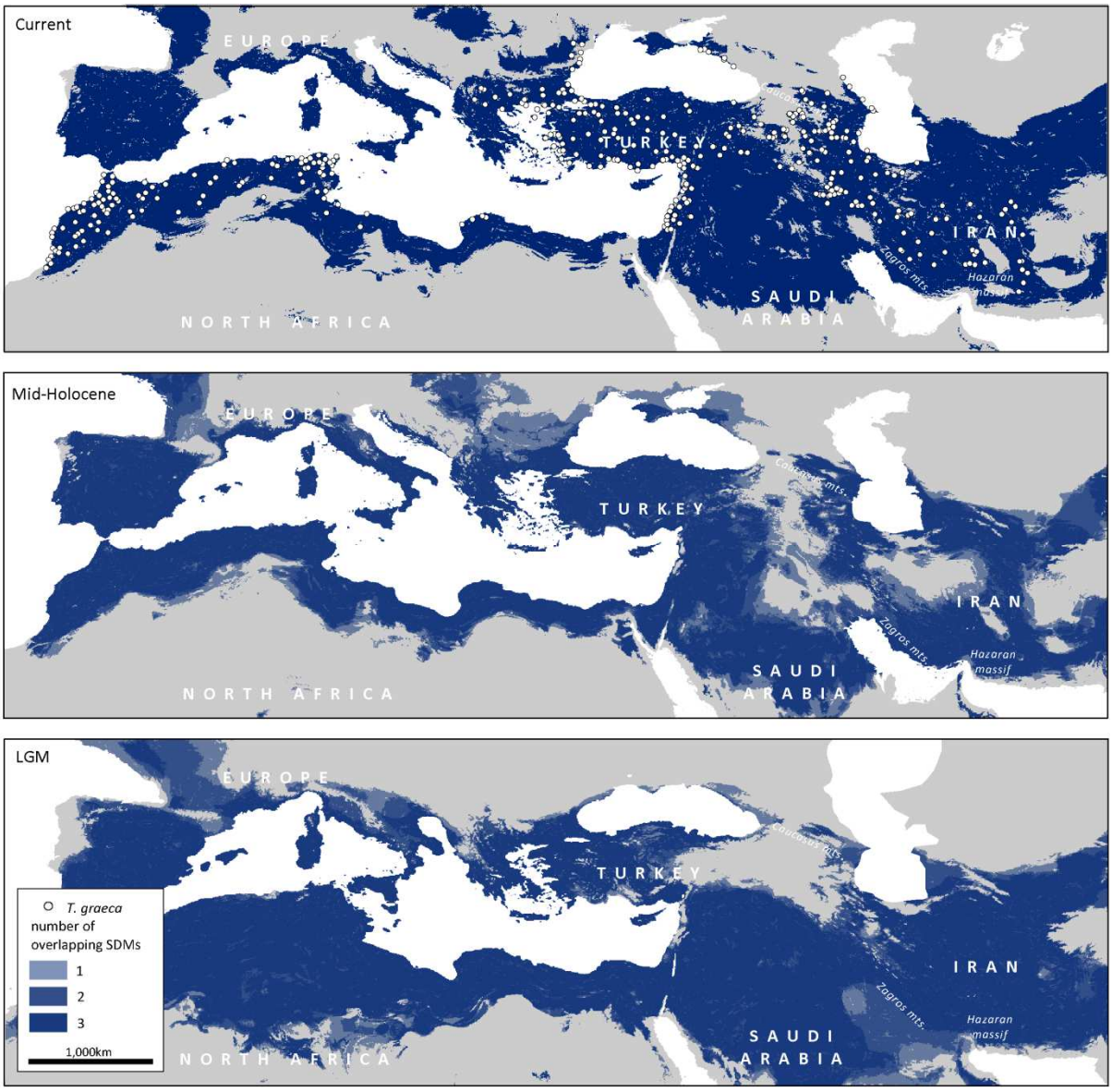

Figure S3 Three-dimensional hypervolumes of the environmental niches for *Testudo graeca.* Circles represent 650 georeferenced occurrence records of *T. graeca* obtained from own field research, scientific publications (Fritz *et al.*, 2007; Parham *et al.* 2012; Mashkaryan *et al.*, 2013) and online databases (GBIF, Vertnet).

Table S1 A list of *Testudo graeca* samples analyzed for cytochrome *b* variation.

Taxon	ID	Locality	Country	X	Y	mtDNA	Reference	GenBank	No. in Fig. 1
T. g. armeniaca	-	Melekli	Turkey	39.95442	44.101543	A	Fritz et al. (2007)	AM230957	-
T. g. armeniaca	-	Beylagan	Azerbaijan	39.718555	47.568544	A	Fritz et al. (2007)	AM230967	-
T. g. armeniaca	-	Beylagan	Azerbaijan	39.718555	47.568544	A	Fritz et al. (2007)	AM230968	-
T. g. armeniaca	-	Beylagan	Azerbaijan	39.718555	47.568544	A	Fritz et al. (2007)	AM230969	-
T. g. armeniaca	-	Kolani	Azerbaijan	41.183635	49.134512	A	Fritz et al. (2007)	AM230975	-
T. g. armeniaca	-	Kolani	Azerbaijan	41.183635	49.134512	A	Fritz et al. (2007)	AM230976	-
T. g. armeniaca	-	Kolani	Azerbaijan	41.183635	49.134512	A	Fritz et al. (2007)	AM230977	-
T. g. armeniaca	-	Dagestanskie Ogni	Russia, Dagestan	42.131119	48.195117	A	Fritz et al. (2007)	AM230978	-
T. g. armeniaca	-	Dagestanskie Ogni	Russia, Dagestan	42.131119	48.195117	A	Fritz et al. (2007)	AM230979	-
T. g. armeniaca	-	Dagestanskie Ogni	Russia, Dagestan	42.131119	48.195117	A	Fritz et al. (2007)	AM230980	-
T. g. armeniaca	-	Novkhani	Azerbaijan	40.539758	49.789389	A	Fritz et al. (2007)	AM230981	-
T. g. armeniaca	-	Zelenomorsk	Russia, Dagestan	42.759314	47.70097	A	Fritz et al. (2007)	AM231000	-
T. g. armeniaca	-	Zelenomorsk	Russia, Dagestan	42.759314	47.70097	A	Fritz et al. (2007)	AM231001	-
T. g. armeniaca	-	Armavir	Armenia	40.15	43.84	A	Mashkaryan et al. (2013)	HF954126	-
T. g. armeniaca	-	Tcobi	Armenia, Nagorno Karabakh	39.02	46.65	A	Mashkaryan et al. (2013)	HF954143	-
T. g. armeniaca	-	Tcobi	Armenia, Nagorno Karabakh	39.02	46.65	A	Mashkaryan et al. (2013)	HF954144	-
T. g. armeniaca	-	Tcobi	Armenia, Nagorno Karabakh	39.02	46.65	A	Mashkaryan et al. (2013)	HF954145	-
T. g. armeniaca	-	Aknyakbur	Armenia, Nagorno Karabakh	39.51	47.02	A	Mashkaryan et al. (2013)	HF954153	-
T. g. armeniaca	-	Nrnadzor	Armenia	38.92	46.43	A	Mashkaryan et al. (2013)	HF954155	-
T. g. armeniaca	-	Nrnadzor	Armenia	38.92	46.43	A	Mashkaryan et al. (2013)	HF954158	-
T. g. armeniaca	5283Jolfa	Jolfa	Iran	38.875645	45.632218	A	this study	KY392819	8
T. g. armeniaca	5303Jolfa	Jolfa	Iran	38.875645	45.632218	A	this study	KY392820	8
T. g. armeniaca	5304Aghcha	Aghchay	Iran	38.833333	44.85	A	this study	KY392821	39
T. g. armeniaca	5305Aghcha	Aghchay	Iran	38.833333	44.85	A	this study	KY392822	39
T. g. armeniaca	5306Aghcha	Aghchay	Iran	38.833333	44.85	A	this study	KY392823	39
T. g. buxtoni	5294aliaba	Aliabad	Iran	33.666667	46.566667	E	this study	KY392825	1
T. g. buxtoni	5295aliaba	Aliabad	Iran	33.66666	46.566667	E	this study	KY392824	1
T. g. buxtoni	5296aliaba	Aliabad	Iran	33.666667	46.566667	E	this study	KY392826	1
T. g. buxtoni	-	between Germi and Razay-Amir Abad	Iran	38.88391	48.012791	E	Fritz et al. (2007)	AM230991	2
T. g. buxtoni	5326Arsanj	Arsanjan	Iran	29.919263	53.297704	E	this study	KY392827	3
T. g. buxtoni	5300Baft	Baft	Iran	29.227279	56.603817	E	this study	KY392828	4
T. g. buxtoni	5331Dehlil	Dehlili	Iran	34.833333	46.55	E	this study	KY392830	5
T. g. buxtoni	5332Dehlil	Dehlili	Iran	34.833333	46.55	E	this study	KY392829	5
T. g. buxtoni	5276divand	Divandare	Iran	35.882718	47.019734	E	this study	KY392832	6
T. g. buxtoni	5277divand	Divandare	Iran	35.882718	47.019734	E	this study	KY392833	6
T. g. buxtoni	5278divand	Divandare	Iran	35.882718	47.019734	E	this study	KY392834	6
T. g. buxtoni	5409divand	Divandare	Iran	35.882718	47.019734	E	this study	KY392831	6

Taxon	ID	Locality	Country	X	Y	mtDNA	Reference	GenBank	No. in Fig. 1
T. g. buxtoni	-	Harzevil	Iran	36.739166	49.429458	E	Parham et al. (2012)	GQ855760	7
T. g. buxtoni	5282Jolfa	Jolfa	Iran	38.875645	45.632218	E	this study	KY392835	8
T. g. buxtoni	5297Kaleji	Kaleji	Iran	38.4	46.866667	E	this study	KY392836	9
T. g. buxtoni	5298Kaleji	Kaleji	Iran	38.4	46.866667	E	this study	KY392838	9
T. g. buxtoni	5299Kaleji	Kaleji	Iran	38.4	46.866667	E	this study	KY392837	9
T. g. buxtoni	5288khomai	Khomain	Iran	33.666667	49.866667	E	this study	KY392839	10
T. g. buxtoni	5289khomai	Khomain	Iran	33.666667	49.866667	E	this study	KY392840	10
T. g. buxtoni	5552Kordab	Kordabad	Iran	32.8	52.416667	E	this study	KY392841	11
T. g. buxtoni	-	Kuhpayeh	Iran	32.717328	52.436555	E	Fritz et al. (2007)	AM230989	12
T. g. buxtoni	-	Lalabad	Iran	34.566667	46.9	E	Parham et al. (2012)	GQ855761	13
T. g. buxtoni	5328Mahida	Mahidasht	Iran	34.25	46.766667	E	this study	KY392842	14
T. g. buxtoni	-	Nowshar near Manjil	Iran	36.735588	49.418159	E	Fritz et al. (2007)	AM230958	15
T. g. buxtoni	-	Meshgin Shahr	Iran	38.448954	47.704971	E	Fritz et al. (2007)	AM230984	16
T. g. buxtoni	-	Meshgin Shahr	Iran	38.448954	47.704971	E	Fritz et al. (2007)	AM230985	16
T. g. buxtoni	5290nazara	Nazarabad	Iran	34.616667	47.516667	E	this study	KY392844	17
T. g. buxtoni	5292nazara	Nazarabad	Iran	34.616667	47.516667	E	this study	KY392845	17
T. g. buxtoni	5293nazara	Nazarabad	Iran	34.616667	47.516667	E	this study	KY392843	17
T. g. buxtoni	-	S Rasht: between Saravan and Rostamabad	Iran	36.950651	49.55422	E	Fritz et al. (2007)	AM230959	18
T. g. buxtoni	-	S Rasht: between Saravan and Rostamabad	Iran	36.950651	49.55422	E	Fritz et al. (2007)	AM230960	18
T. g. buxtoni	-	S Rasht: between Saravan and Rostamabad	Iran	36.950651	49.55422	E	Fritz et al. (2007)	AM230961	18
T. g. buxtoni	-	Sefid Rud	Iran	37.368924	48.147061	E	Fritz et al. (2007)	AM230962	19
T. g. buxtoni	5280sepida	Sepidan	Iran	30.20066	51.986526	E	this study	KY392846	20
T. g. buxtoni	5285shahre	Shahrekord	Iran	32.35	50.366667	E	this study	KY392848	21
T. g. buxtoni	5287shahre	Shahrekord	Iran	32.35	50.366667	E	this study	KY392847	21
T. g. buxtoni	5541Sultan	Sultanabad	Iran	37.316667	45.25	E	this study	KY392849	22
T. g. buxtoni	5542Sultan	Sultanabad	Iran	37.316667	45.25	E	this study	KY392850	22
T. g. buxtoni	5543Sultan	Sultanabad	Iran	37.316667	45.25	E	this study	KY392851	22
T. g. buxtoni	5307Islama	Islamabad	Iran	34.266667	46.266667	E	this study	KY392852	23
T. g. buxtoni	5314Ahar	Ahar	Iran	38.766667	46.866667	E	this study	KY392853	24
T. g. buxtoni	5315Niyaz	Niyaz	Iran	38.383333	47.916667	E	this study	KY392854	25
T. g. buxtoni	5540Siyahd	Siyahdare	Iran	34.766667	47.233333	E	this study	KY392855	26
T. g. buxtoni	5544Kuzera	Kuzerash	Iran	45.25	38.183333	E	this study	KY392856	27
T. g. buxtoni	5546Kuzera	Kuzerash	Iran	45.25	38.183333	E	this study	KY392857	27
T. g. buxtoni	5553Nahoj	Nahoj	Iran	32.916667	52.633333	E	this study	KY392858	28
T. g. buxtoni	-	East Azerbaijan Province	Iran	37.54	46.16	E	Mashkaryan et al. (2013)	HF954160	29
T. g. buxtoni	-	Zanjan	Iran	36.70	48.29	E	Mashkaryan et al. (2013)	HF954161	30
T. g. zarudnyi	-	Anjir Avand	Iran	32.500361	54.433588	F	Fritz et al. (2007)	AM230983	31
T. g. zarudnyi	-	Shahr-e-Babak	Iran	30.118817	55.118367	F	Fritz et al. (2007)	AM230987	36
T. g. zarudnyi	-	Saghand	Iran	32.550316	55.221475	F	Fritz et al. (2007)	AM230998	35

Taxon	ID	Locality	Country	X	Y	mtDNA	Reference	GenBank	No. in Fig. 1
T. g. zarudnyi	-	Neyriz	Iran	29.201254	54.322955	F	Fritz et al. (2007)	AM230986	32
T. g. zarudnyi	5270Baft	Baft	Iran	29.227279	56.603817	F	this study	KY392861	4
T. g. zarudnyi	-	Shahr-e-Babak	Iran	30.118817	55.118367	F	Fritz et al. (2007)	AM230988	36
T. g. zarudnyi	-	Tabas	Iran	33.590402	56.937407	F	Fritz et al. (2007)	AM230999	37
T. g. zarudnyi	-	Kuh-e Taftan	Iran	28.60863	61.133299	F	Parham et al. (2012)	GQ855762	38
T. g. zarudnyi	5274Rabor	Rabor	Iran	29.289155	56.913084	F	this study	KY392865	34
T. g. zarudnyi	5275Rabor	Rabor	Iran	29.289155	56.913084	F	this study	KY392866	34
T. g. zarudnyi	5302Baft	Baft	Iran	29.227279	56.603817	F	this study	KY392860	4
T. g. zarudnyi	5549Nir	Nir	Iran	31.501176	54.138668	F	this study	KY392862	33
T. g. zarudnyi	5550Nir	Nir	Iran	31.501176	54.138668	F	this study	KY392863	33
T. g. zarudnyi	5551Nir	Nir	Iran	31.501176	54.138668	F	this study	KY392864	33
T. g. zarudnyi	-	Nir	Iran	31.501176	54.138668	F	Fritz et al. (2007)	AM230990	33
T. g. zarudnyi	5301Baft	Baft	Iran	29.227279	56.603817	F	this study	KY392859	4